MPDA
Master's degree
Parametric Design in Architecture

UNIVERSITAT POLITÈCNICA DE CATALUNYA
BARCELONATECH
School of Professional & Executive Development

Post-Optimization of a Single-Layer Elastic Gridshell

Julien ROBINET, Hsiang-Yi LEE, Michael RAUCH

Abstract

This study falls within the scope of research dedicated to the design of small-scale elastic gridshells made of timber. A single-layer gridshell is presented, which was built in an academic framework during the Master of Parametric Design in Architecture at the Universitat Politècnica de Catalunya. It is studied how far its structural performance can be improved while maintaining the simplicity of single-layer gridshells and avoiding extensive designs of the nodes. Therefore, advanced computational tools are applied to develop optimization algorithms to generate efficient patterns for the bracing and the second layer.

Keywords: Chebyshev, elastic gridshell, bracing, efficiency, structural optimization, structural performance.

1. Introduction

For their capacity to combine lightness and structural performance elastic gridshells are appealing to both architects and engineers [1]. They are composed of a planar grid of initially straight continuous elements, bent progressively into their final shape [2], which usually has double curvature. Therefore such structures benefit from the property that the stresses are mainly transmitted through compression and tension. The elements are pinned together so that the grid has no in-plane shear stiffness and allows large-scale deformations during erection. After the erection, the deformed grid needs to be braced to lock the shape and to ensure the shear stiffness of the structure. To increase the structural performance, e.g. the ability to withstand external loads, elastic gridshells are often arranged in superposed layers. The curvature and thus the permissible bending radii limit the cross-sectional dimensions of the individual layers.

Such systems were developed by Frei Otto in the 1970s, e.g. the Multihalle Mannheim. Since then the principles of elastic gridshells have been studied and used in several projects to achieve innovative architectural forms (see Chapter 2).

There are several building systems of elastic gridshells, each associated with specific structural and geometrical characteristics. The corresponding meshes represent the arrangement of the profiles. One of them are Chebyshev meshes that are composed exclusively of equal-length quadrilaterals. This building system is the core of this paper and the basis for the following considerations.

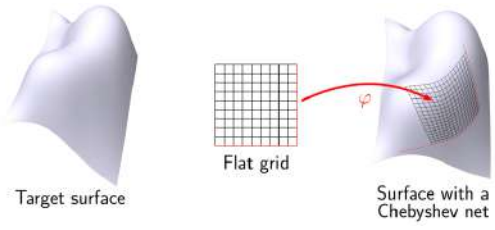

Figure 1: Chebyshev net on a target surface [3].

1.1. Motivation

Due to the initial planar grid, the erection process of elastic Chebyshev gridshells is simple and fast. Continuous and repetitive profiles as well as the low complexity of the nodes, which usually consist of a single bolt, lead to an efficient and economic design.

However, bracing the structure after the erection is time-consuming and inefficient, which makes it valuable to optimize the bracing in order to reduce it to a minimum. This saves material and also construction time.

The load-bearing profiles of single-layer elastic gridshells usually have a low moment of inertia and thus a limited capacity to withstand external loads. Additional layers are added to increase the resistance of the structure, which also leads to a significant increase in weight. This can be a considerable constraint in terms of erection. The nodes of elastic gridshells with additional layers are designed so as to allow a certain sliding between the profiles during the erection process. This is either achieved by adding slotted holes, which is locally weakening the profiles, or by an extensive design of the nodes, which requires an elaborate and cost-intensive fabrication.

Therefore, the question arises of how far it is advantageous to add additional layers to a small-scale elastic gridshell, or whether it can be beneficial to reinforce only certain areas.

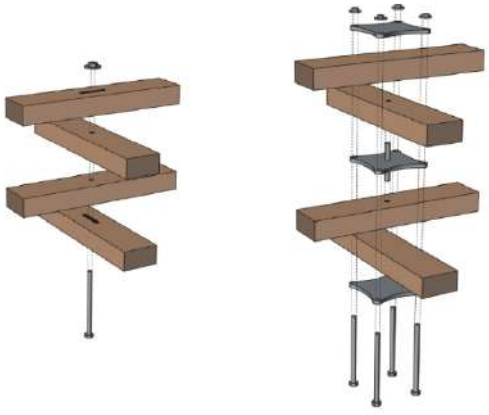

Figure 2: Nodes of a double-layer grid: slotted holes (left), clamping plate (right) [4].

1.2. Research Aim

In this paper, we investigate efficient patterns for adding short elements of the bracing and the additional layer, aiming to keep the simplicity of single-layer elastic gridshells by reinforcing only certain areas after the erection.

2. State of the Art

Following, several notable projects are examined for their bracing and reinforcing strategies.

2.1. Toledo Gridshell 2.0, Italy, by University of Naples Federico II (2015)

The gridshell is composed of straight and continuous timber laths, elastically bent into a double curvature form. The flat grid was first assembled on the ground, with a second layer applied everywhere. This leads to high weight and requires the use of special machinery for the erection process. The gridshell is braced with short sticks as diagonals. These are added in every second

rhombus of the grid with a chessboard-like pattern in an intermediate layer between the first and second layers. Each rhombus has a diagonal of a different length. Therefore, the sticks are divided into three individual segments of different lengths. This ensures repetitive elements and overlapping margins during the assembly process, which makes them easy and fast to assemble [5].

- Bracing: Short sticks (optimized globally)
- Boundary beams: Same cross-section as the grid
- Second layer: Everywhere applied

2.2. Portalen Pavilion, Sweden, by Map13 Barcelona, Summum Engineering, and Edyta Augustynowicz (2019)

The gridshell was built to serve as a meeting and event space for the community center. It is composed of a double-layer grid, whereas the large openings are reinforced with stiff boundary beams made of glulam. This allows the grid to be sufficiently braced with only a few cables of small diameter. The grid is covered with polycarbonate sheets [6].

- Bracing: Cables (optimized globally)
- Boundary beams: Stiff glulam beams
- Second layer: Everywhere applied

2.3. Accoya Gridshell, Australia, by Melbourne School of Design and Gridshell.it (2014)

The gridshell was built in an academic framework as part of the "Issues in Technology" workshop. It is diagonally braced with long continuous laths arranged in a square grid with varying rotations and offsets. The pattern of the bracing is optimized using evolutionary algorithms in order to minimize the curvature of each element. The outer bracing is composed of double-layer beams, whereas the inner bracing consists of single beams [7].

- Bracing: Long continuous beams (optimized globally)
- Boundary beams: Not applied
- Second layer: Everywhere applied

2.4. Trebesov Gridshell, Czech Republic, by Unizono and Matrix a.s. (2016)

The hyperboloid gridshell was built in a public park and is mainly used for cultural and social events. It is composed of a single-layer grid, which reduces the overall weight and allows for an effortless erection. To provide sufficient stiffness, it is braced with a hybrid system of cables and beams. The cables are uniformly distributed in every fourth rhombus, whereas long continuous beams are locally added on top of the gridshell to provide further reinforcement. The openings are reinforced with double-layer beams. [8].

- Bracing: Cables (optimized globally), long continuous beams (optimized locally)
- Boundary beams: Double-layer beams
- Second layer: Not applied

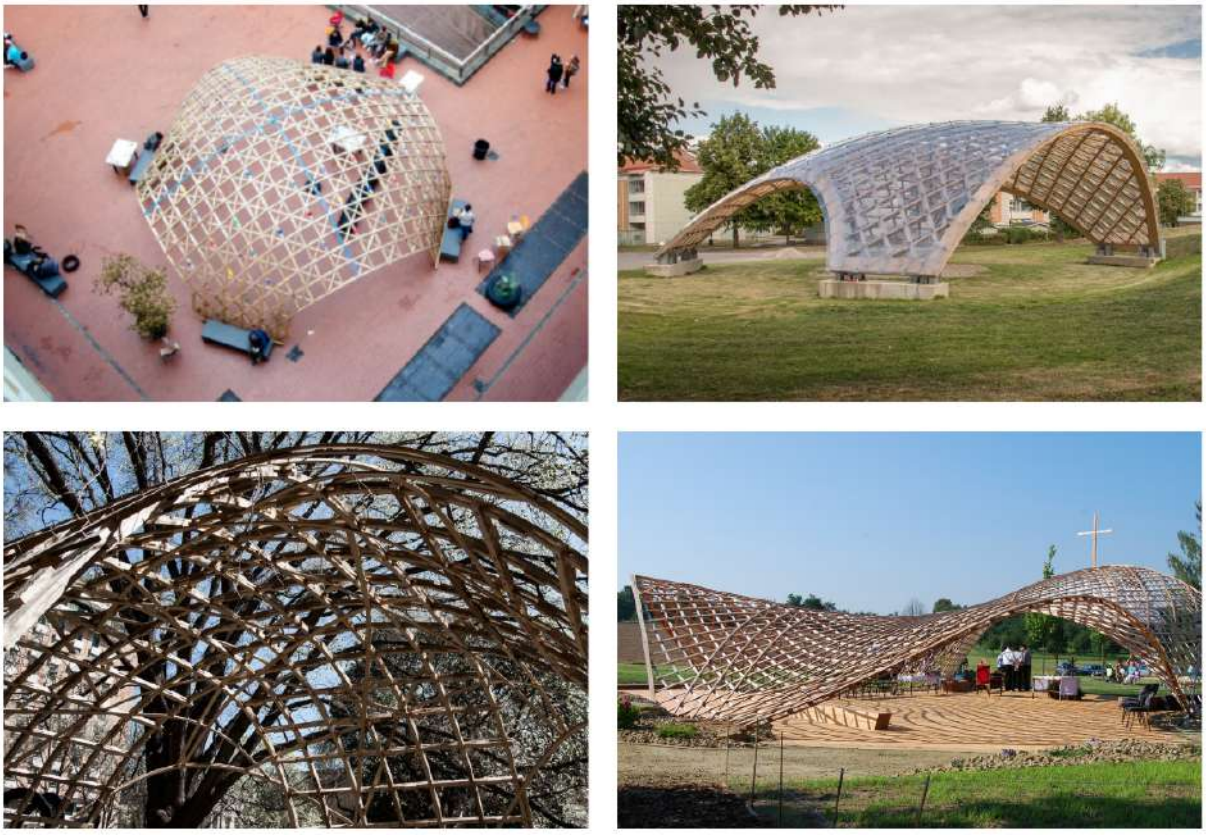

Figure 3: Toledo Gridshell 2.0 (top left); Portalen Pavilion (top right); Accoya Gridshell (bottom left); Trebesov Gridshell (bottom right).

3. Methodology

In Chapter 3.1. the single-layer elastic gridshell is introduced which is the basis for the following optimization. This highlights the most important assumptions and steps during the design process that led to the as-built structure. Chapter 3.2. presents in detail the individual optimization algorithms and compares intermediate results. Finally, in Chapter 3.3. different combinations of these algorithms are built and final results are discussed.

3.1. Case Study

Figure 4: Gridshell built at the campus of the Escuela Técnica Superior de Arquitectura del Vallés (ETSAV).

The gridshell was designed and built during the second semester of the Master of Parametric Design in Architecture at the Universitat Politècnica de Catalunya. It is erected at the campus of the Escuela Técnica Superior de Arquitectura del Vallés (ETSAV) and covers an area of around 83,0 m². It follows the principles of the building system of Chebyshev gridshells with constant edge length.

The straight continuous beams are made of birch plywood with a thickness of 21 mm and a width of 50 mm. They are assembled of discrete segments with an individual length of 3,05 m. According to the manufacturer's data from the *Handbook of Finnish Plywood* [9], the main material properties are as follows:

Table 1: Main material properties for t = 21 mm

	Characteristic strength			Mean modulus of elasticity	
Density [kg/m³]	Bending [N/mm²]	Compression [N/mm²]	Tension [N/mm²]	Bending [N/mm²]	Tension/Compression [N/mm²]
680	$f_{m\,II} = 39,4$ $f_{m\,\perp} = 34,3$	$f_{c\,II} = 27,0$ $f_{c\,\perp} = 25,0$	$f_{t\,II} = 39,0$ $f_{t\,\perp} = 36,0$	$E_{m\,II} = 9858$ $E_{m\,\perp} = 7642$	$E_{t/c\,II} = 9093$ $E_{t/c\,\perp} = 8407$

3.1.1. Form Finding

The grid pattern results from an iterative process, where an initially flat grid with an edge length of 0,74 m is vertically pulled towards a target surface. The surface has double curvature and serves as a geometrical reference. The corresponding curve network is then cut with the xy plane and geodesic curves at the openings. Geodesic curves have the property of having no geodesic but only normal curvature. Consequently, the beams at the openings can be effortlessly attached after the grid has been erected. The height at the openings measures 2,6 m whereas the central height measures 3,4 m. The span between the supports varies from 7,6 m to 9,8 m.

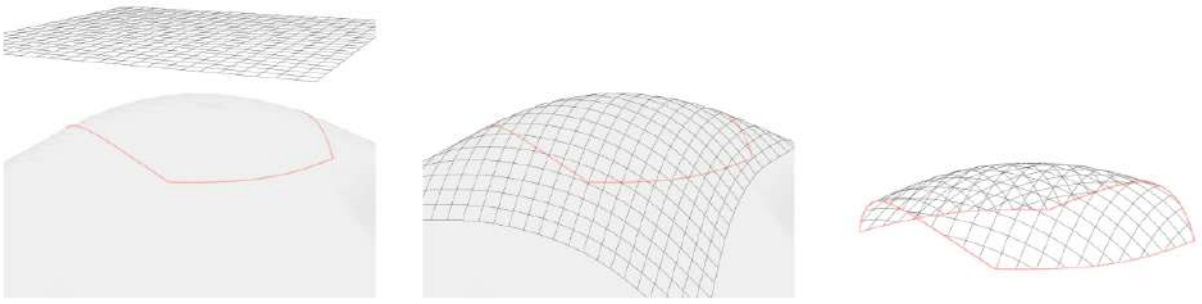

Figure 5: Flat grid; curve network on target surface; curve network cut with the xy plane and geodesic curves.

3.1.2. Curvature

Due to the bending process, high stresses are introduced to the beams. It is therefore crucial to optimize the grid pattern so that the curvature of the beams and consequently the initial bending stresses are reduced. As these stresses can be determined with the Euler-Bernoulli law [10]

$$\frac{1}{r} = \frac{M}{E \cdot I} \tag{1}$$

it can be written as an expression of the section modulus W, the modulus of elasticity E, the curvature $1/r$ and the thickness of the beams:

$$\sigma = \frac{E \cdot I}{r \cdot W} = \frac{E \cdot t}{2 \cdot r} \tag{2}$$

This results in a minimum bending radius that can be achieved with certain material properties and dimensions:

$$r_{min} = \frac{E \cdot t}{2 \cdot \sigma} \tag{3}$$

With this approach, both normal and geodesic curvature are controlled separately. The following figure compares the bending radii of the beams with a minimum bending radius for 20% to 70% of material strength.

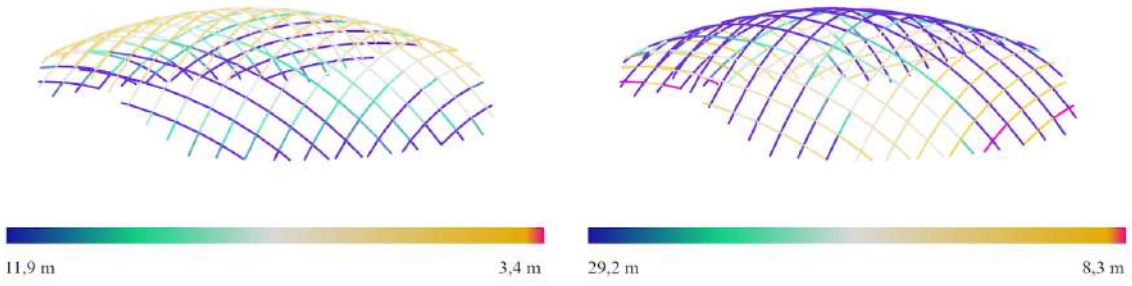

Figure 6: Analysis of the normal (left) and geodesic (right) curvature by comparing the bending radii.

This approach is a simplified approximation since it does not take into account the interaction of both curvatures or other phenomena such as torsion. It is nevertheless useful for a quick estimation of the material utilization during the design process.

To achieve more accurate results, the structure is modeled with the help of the Kiwi!3D, a plug-in within the Grasshopper environment, which is based on isogeometric analysis (IGA). Through embedded non-linear analysis, it is also possible to simulate the shape that the structure will take after the bending process.

The following figure shows the utilization of the beams due to the introduced stresses during the bending process for the grid forced into the desired shape and its relaxed shape.

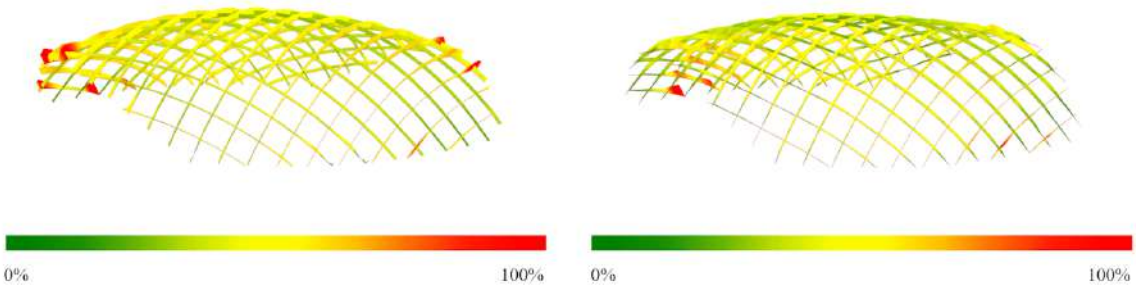

Figure 7: Utilization due to introduced stresses during bending; forced shape (left); relaxed shape (right).

3.1.3. Structural System

With Karamba3D, a structural engineering tool embedded in Grasshopper, the beams are modeled with the aforementioned cross-section and material as a single-layer gridshell. The supports are defined so as to prevent translation in all axes. Whereas the rotation around the local z-axis is locked, the rotation around the local x-axis and y-axis is released.

To provide shear stiffness to the structure, additional bracing elements are required, which triangulate the grid. This reduces the displacement due to external loads but also ensures that the structure takes its desired shape after the bending process. Usually, cables or rigid elements are chosen for this purpose. One advantage of rigid elements is that they can take both tension and compression, whereas cables can only take tension. Consequently, the quadrilaterals do not necessarily need to be braced in both directions. The built structure is horizontally braced with continuous timber laths of the same cross-section and material as the beams.

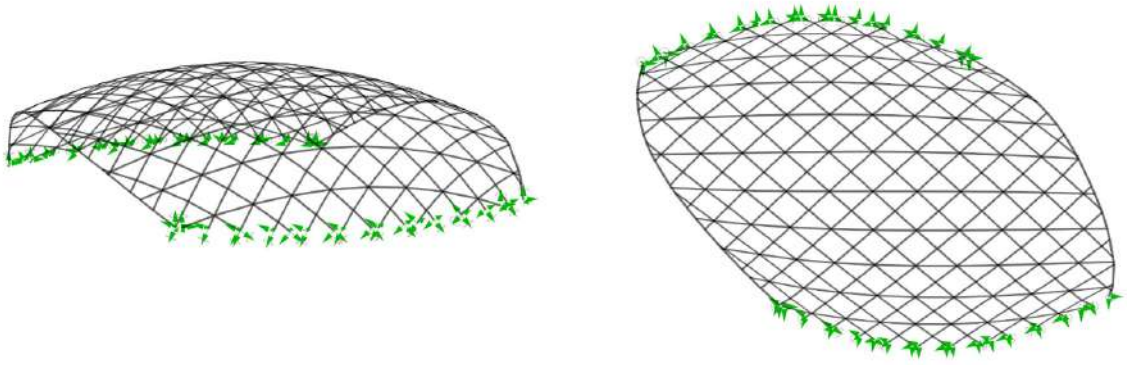

Figure 8: Structural system with defined supports.

The openings are reinforced with boundary beams following the geodesic curves. To increase the stiffness of these beams, i.e. to increase their moment of inertia, they are made of two layers connected with shear blocks. This is considered through modeling these beams with rectangular cross-sections that have the same area and moment of inertia as the corresponding beams with two layers.

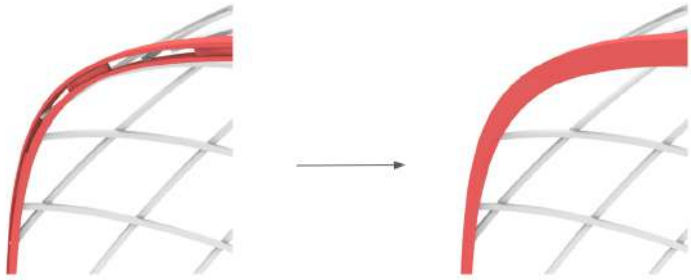

Figure 9: Double-layer boundary beam and its equivalent rectangular cross-section.

Assuming full shear transfer between the two layers, the moment of inertia is calculated as:

$$I_u = 2 \cdot \left[\frac{b \cdot t^3}{12} + b \cdot t \cdot d^2\right] \tag{4}$$

This represents the theoretical upper limit. The theoretical lower limit is calculated as:

$$I_l = 2 \cdot \frac{b \cdot t^3}{12} \tag{5}$$

The actual value is between these two limits and depends on a calibrating factor α, that accounts for the physical distribution and the rigidity of the joints. It follows:

$$I_e = 2 \cdot \frac{b \cdot t^3}{12} + \alpha \tag{6}$$

In this research, I_e is considered to be the mean value of I_u and I_l assuming 50% of shear transfer. For the resulting moment of inertia, an equivalent rectangular cross-section is defined. For the built boundary beams of 50/21 mm connected with shear blocks of 42 mm height, this results in a cross-section of 25/84 mm.

3.1.4. Loads

The loads are applied according to the Eurocode, assuming a membrane to be attached. For the area of Barcelona, the wind load is considered with w_k = 0,53 kN/m² and reduced by a factor of 0,5 for structures that only exist temporarily. The values for pressure and suction are calculated from the Voronoi area, which is assigned to each vertex of the mesh. The most unfavorable wind direction is identified depending on the corresponding structural analysis. The snow load is given as 0,41 kN/m². It is reduced by a factor of 0,8 according to the angle of inclination. The self-weight is automatically calculated based on the specified density.

Within the following structural analysis, the initial stresses caused by the bending process are not applied. Due to the stress relaxation phenomenon of wood, these stresses decrease very quickly during the first weeks. Depending on the curvature radius, they can decrease by 66% of their initial value after two years [11]. Therefore, it can be considered to be a long-term analysis, while keeping a certain capacity for the utilization of the beams.

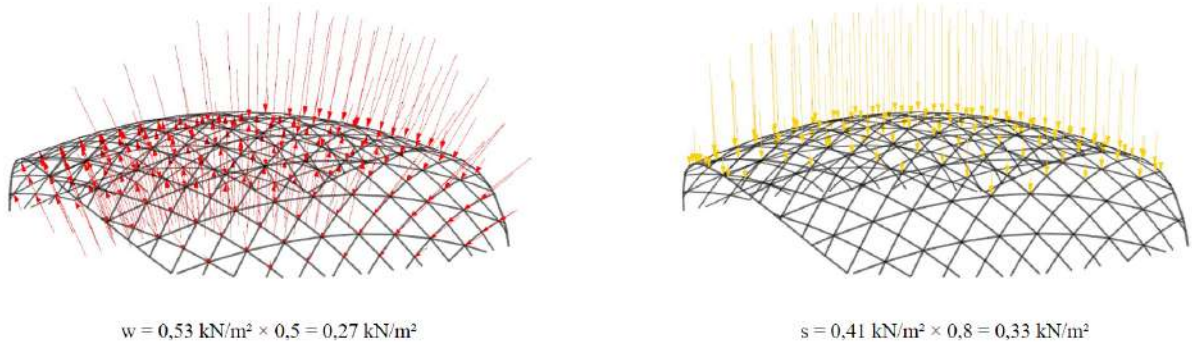

Figure 10: Applied wind and snow loads.

3.1.5. Structural Analysis

Figure 11 shows the max. utilization as well as the max. displacement of the built structure under the aforementioned loads for the most unfavorable wind direction. The utilization is calculated as the ratio between the stresses in the beams and the yield stress of the material. The permissible limit of displacement is defined within a range of *L/100* and *L/200*. For the given span, this is around 8,0 cm to 4,0 cm.

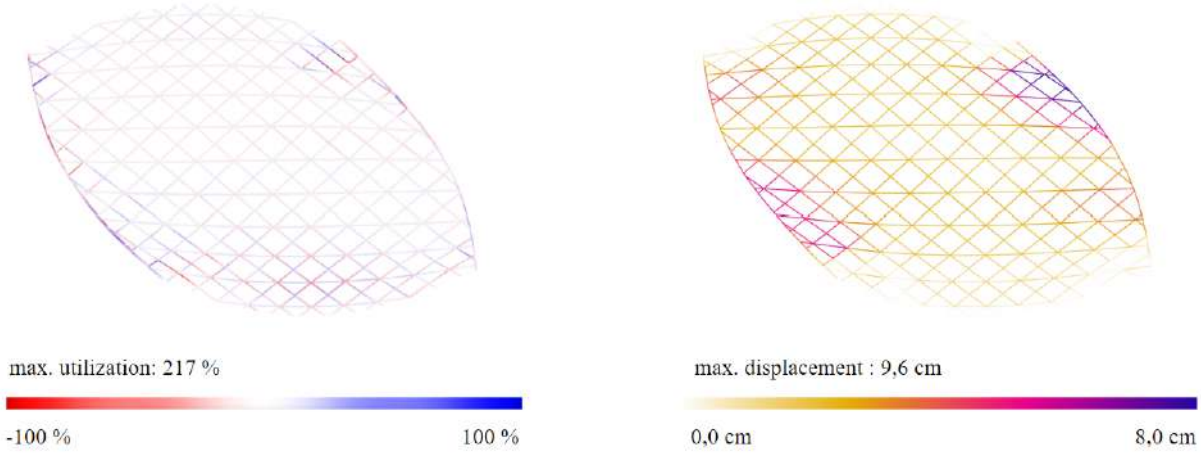

Figure 11: Utilization and displacement of the built structure under the applied loads.

Both the utilization and the displacement exceed the defined limits. For the utilization, a maximum value of 70 % is accepted in order to keep a certain capacity for the initial stresses due to the bending process. Therefore, the structure is optimized in the following chapters. It is studied how the performance can be increased by applying more efficient bracing patterns and by adding second layers to the grid. Also, the impact of increasing the stiffness of the boundary beams is taken into account.

Figure 12 shows the impact of the individual members on the structural behavior and compares the improvement in performance relative to the applied mass. It can be clearly seen that the boundary beams (BB) and the bracing (BR) significantly reduce the utilization and the displacement with 26,0

kg and 78,0 kg of additional weight. This brief comparison already highlights the effectiveness of the boundary beams as reinforcing members.

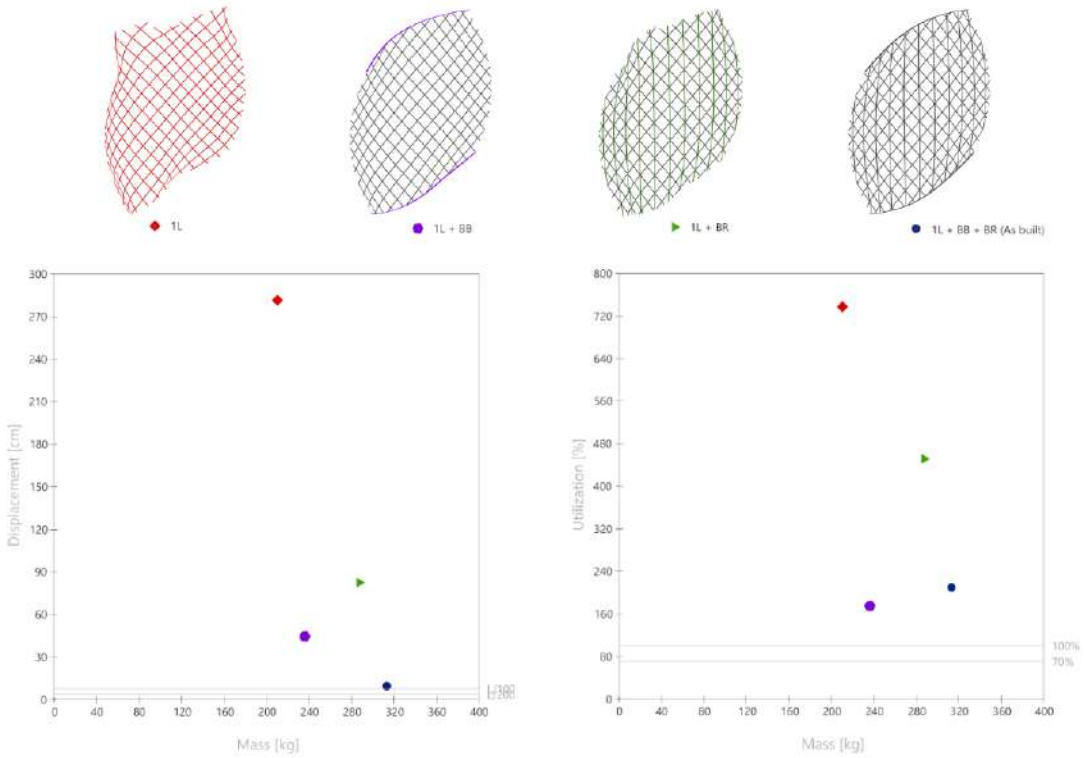

Figure 12: Impact of the individual members on the utilization and the displacement relative to the applied mass.

In addition, comparing the individual members with the workload that is needed for the construction, one can see that the boundary beams are also very fast compared to the bracing, the assembly, and the erection of the grid. The values are based on experience during the construction.

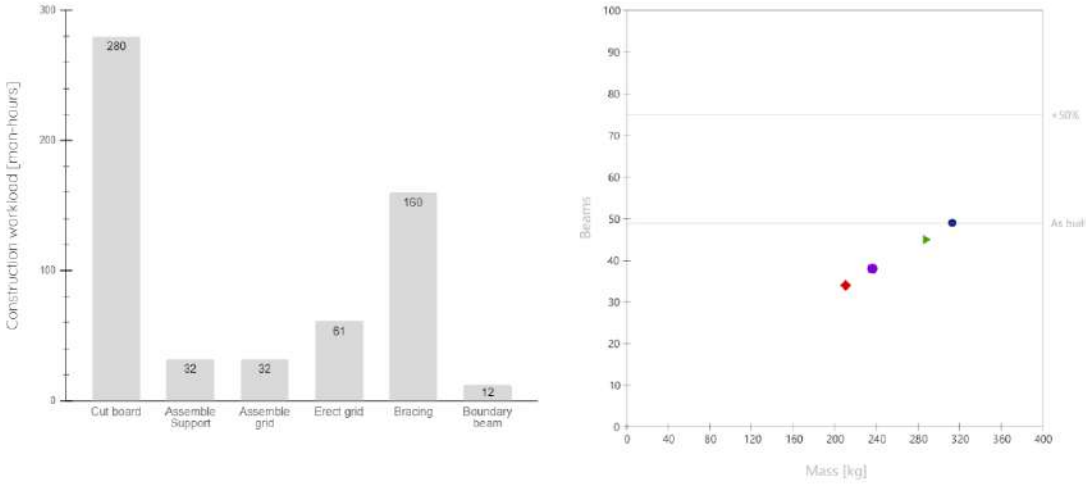

Figure 13: Workload for the construction of the individual members; Comparison of mass to beams.

3.2. Optimization Process and Algorithms

Following, the optimization of the individual members is performed separately and the improvement of the structural performance is investigated.

In advance, the displacement of the built structure is determined considering all possible wind directions. Taking the average of these values, it can be identified where the structure needs to be reinforced the most in terms of displacement. It can be seen that by considering all possible wind directions the built structure still deforms most near the openings.

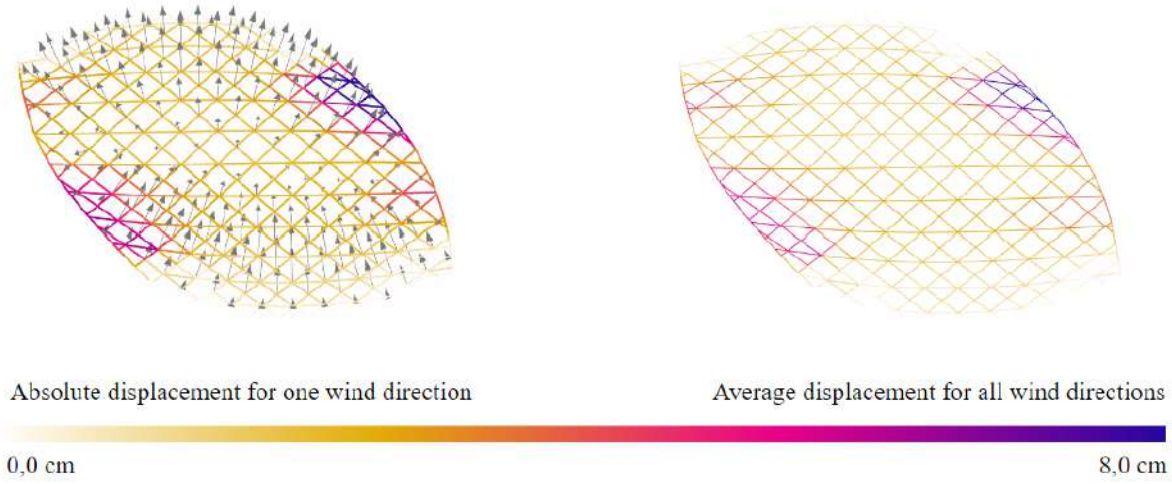

Figure 14: Absolute displacement for one wind direction; Average displacement for all wind directions.

3.2.1. Boundary Beam Optimization

The stiffness of the boundary beams is progressively increased by changing their height. For this a simple algorithm is defined, that increases the boundary beams by 0,5 cm within every loop. The loop stops when either the limit of displacement or the maximum height is reached. A detailed flowchart of this algorithm can be reviewed in Appendix A.1.

Figure 15 shows how the displacement decreases relative to the increased mass of the boundary beams for the single-layer grid without any bracing. At first, the boundary beams are very effective. The curve falls very steeply until it reaches a point where it remains almost straight. Here the maximum displacement shifts from the openings towards the inside of the grid.

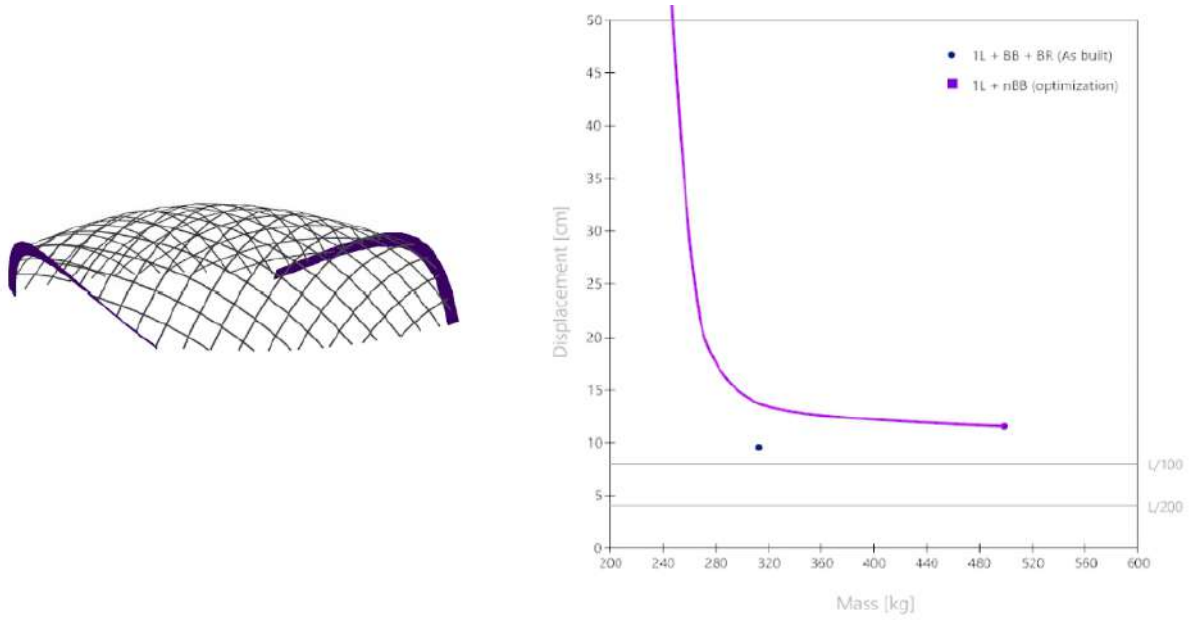

Figure 15: Impact of the boundary beams on the displacement by increasing their stiffness.

3.2.2. Bracing Optimization

For the bracing optimization, an algorithm is developed that is made of two loops.

Within the first loop, the single-layer grid is considered to be fully braced. The average utilization of each bracing element is determined from all possible wind directions (Figure 16). Following, the bracing elements are sorted according to this average. It is expected that these elements with the highest utilization, also have the greatest impact on reducing the displacement.

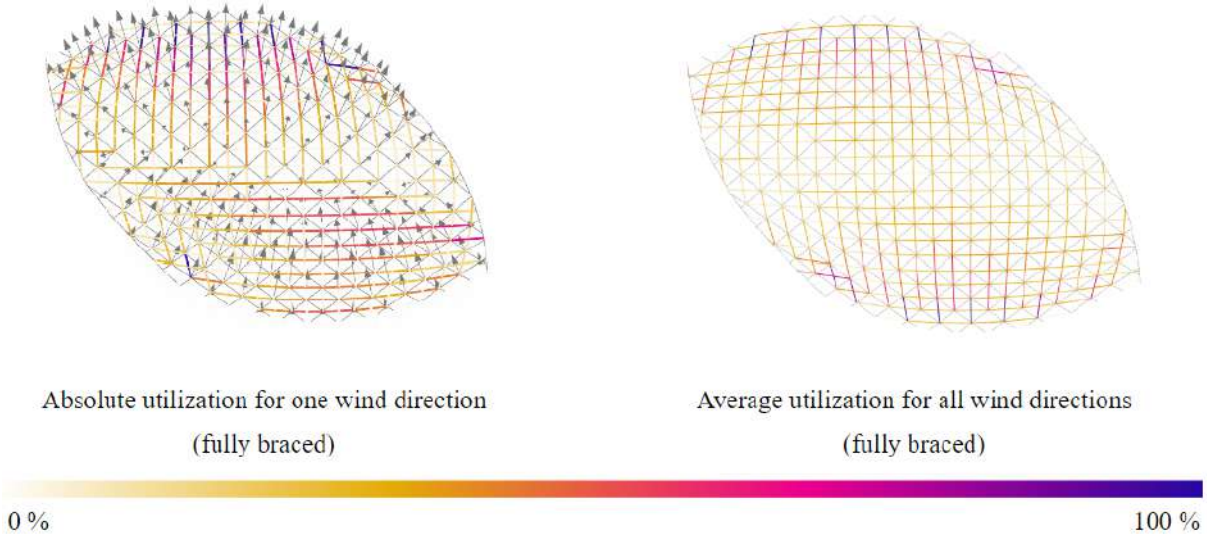

Figure 16: Utilization of all the bracing elements within the first loop.

Considering only the vertical bracing, the highest utilized elements are the ones near the supports. Taking into account only the horizontal bracing, a pattern emerges that has rotational symmetry. Combined, an intersection of these two becomes apparent.

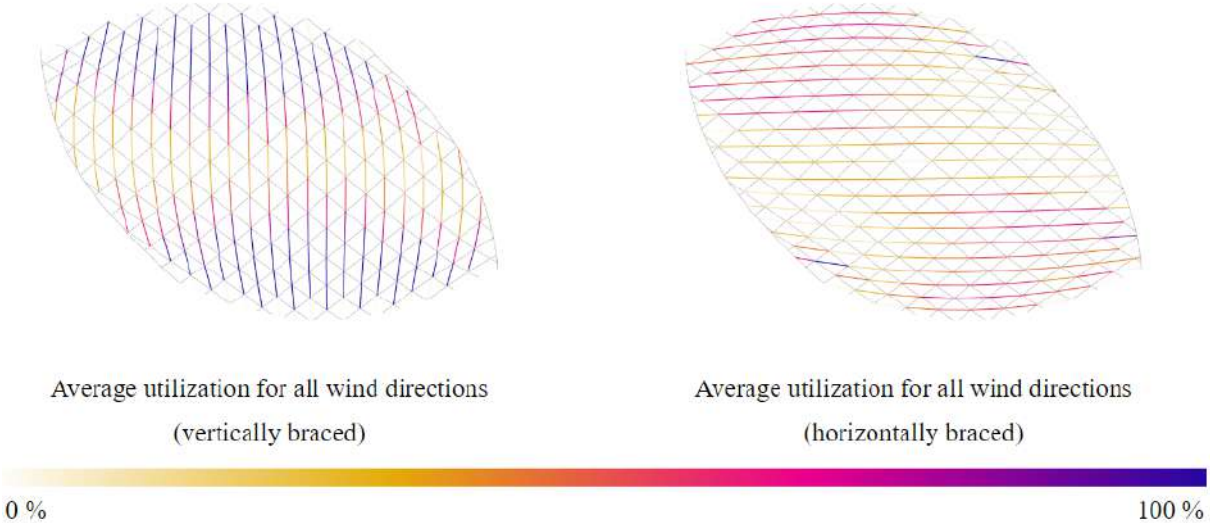

Figure 17: Utilization of the bracing elements individually for the vertical and horizontal directions.

Within the second loop, the bracing elements are added sequentially out of the sorted list from the first loop. It starts with the one that has the highest utilization and stops when either the limit of displacement is reached or no bracing element remains. A detailed flowchart of this algorithm can be reviewed in Appendix A.2.

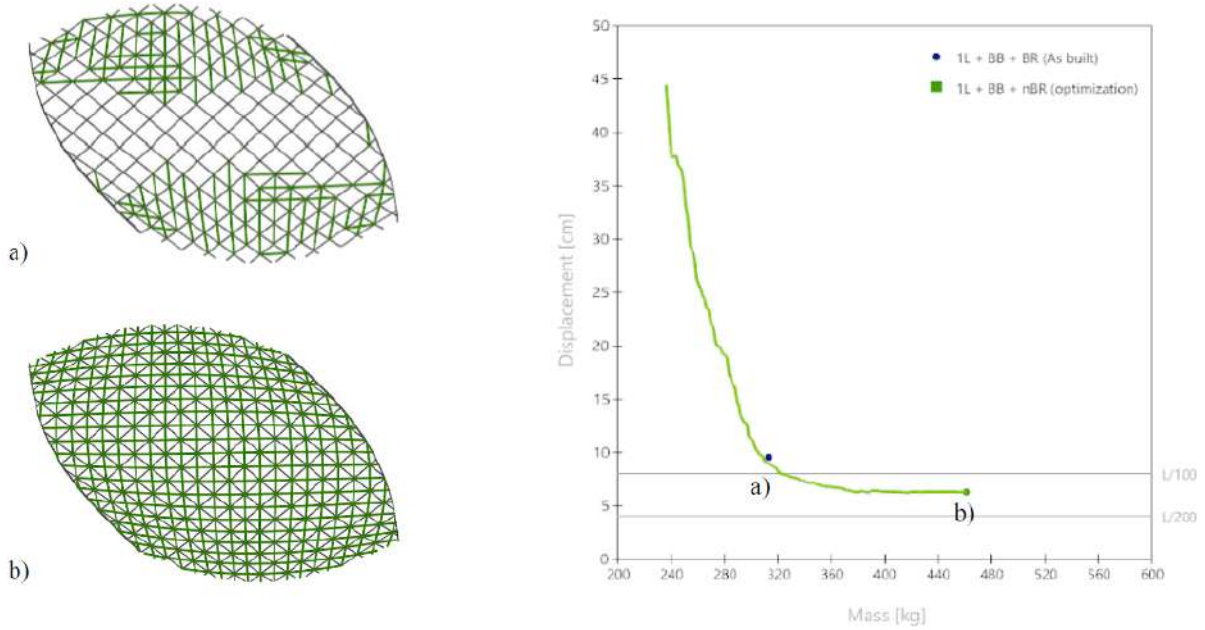

Figure 18: Impact of the bracing on the displacement by adding the elements sequentially; a) optimized pattern at the inflection point; b) fully braced

Figure 18 shows the principle of the second loop. It illustrates the impact of the bracing on the displacement by adding the elements sequentially. Thereby, the displacement is determined for the most unfavorable wind direction. Similar to the boundary beam, the bracing tends to be very effective at first, until it reaches point a) where adding more of the elements is relatively ineffective.

3.2.3. Second Layer Optimization

For the optimization of the second layer, an algorithm is developed similar to the one for bracing. Within the first loop, starting from a single-layer grid without any bracing, the average utilization for each element is determined from all possible wind directions. A pattern emerges where the highest utilized elements tend to be inside the grid arranged in two patches (Figure 19).

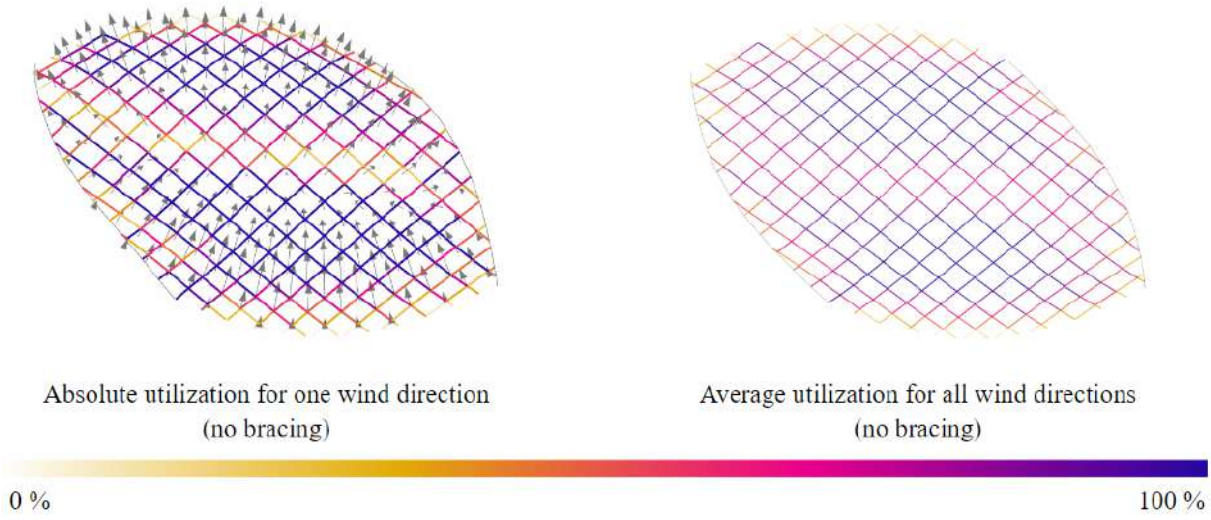

Figure 19: Utilization of all the single-layer elements within the first loop with no bracing applied.

Starting from a single-layer grid that is braced as built, the highest utilized elements shift towards the supports, whereas the bracing takes the utilization inside the grid. Considering the grid to be fully braced, the highest utilized elements tend to move near the openings (Figure 20).

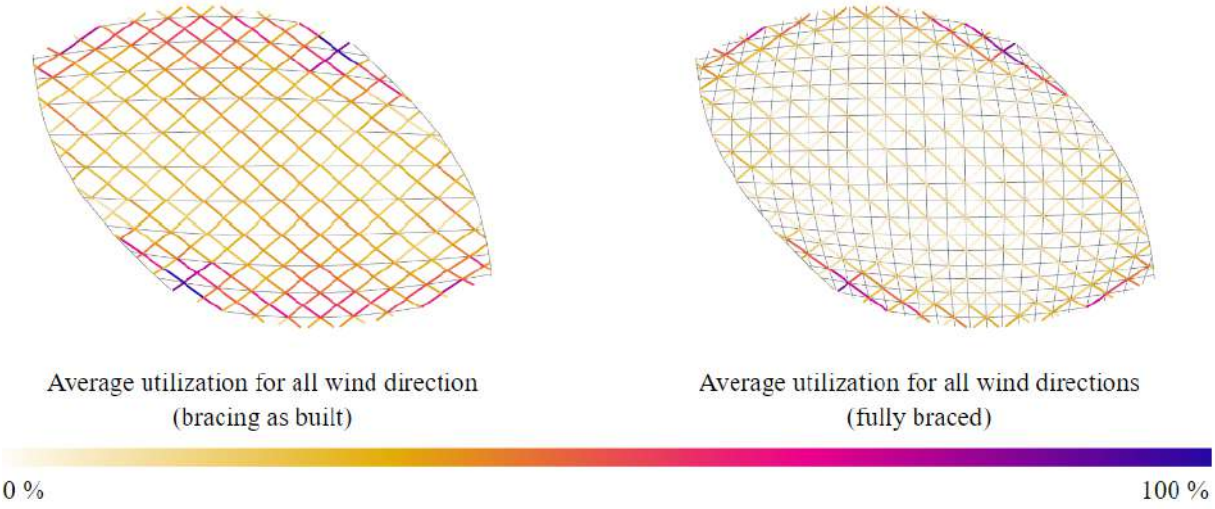

Figure 20: Utilization of all the single-layer elements within the first loop with different bracings.

The elements are then sorted according to this average and sequentially "doubled" starting from the one that has the highest utilization. This is considered through modeling these elements with rectangular cross-sections that have the same area and moment of inertia as the corresponding element with two layers (see Chapter 3.1.3).

The loop stops when either a global utilization of 70% is reached or all beams are "doubled". A detailed flowchart of this algorithm can be reviewed in Appendix A.3.

Figure 21 illustrates the impact of the second layer on the displacement for a single-layer grid without any bracing by "doubling" the elements sequentially. Thereby, the displacement is determined for the most unfavorable wind direction. It can be seen that the displacement is decreasing almost constantly by increasing the inertia of each element.

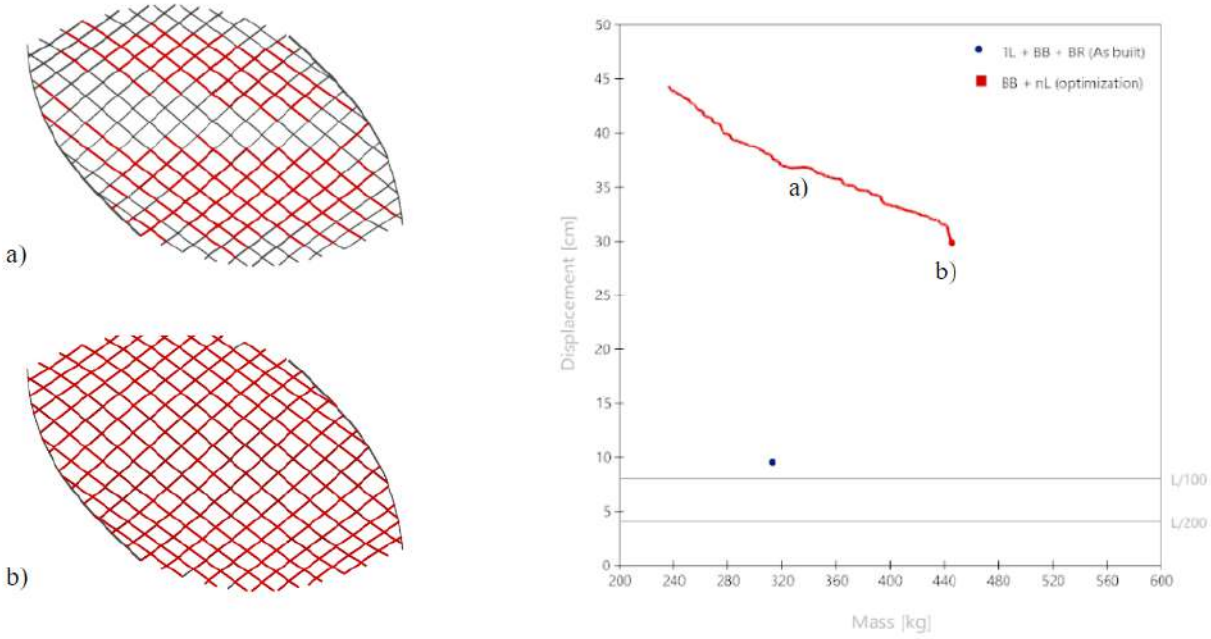

Figure 21: Impact of the second layer on the displacement by "doubling" the elements sequentially; a) optimized pattern at around 50% of the elements; b) 100% of the elements.

3.2.4. Intermediate Comparisons

After these individual investigations, it can be compared and summarized that for the displacement, the boundary beams are very effective at first, up to a point where increasing the stiffness doesn't have much of an impact. The maximum displacement then shifts from the openings towards the inside of the grid.

The bracing is very effective up to around 50% of the potentially available mass. Comparing the performance of the built structure, one can see that the built bracing is already performing very efficiently. Increasing the stiffness of the grid by adding second layers is decreasing the displacement in general, but not as efficient as the boundary beams or the bracing. Individually, with none of these members the maximum limit of displacement (*L/200*) is met.

Figure 22 is comparing the impact of the individual members on the structural performance.

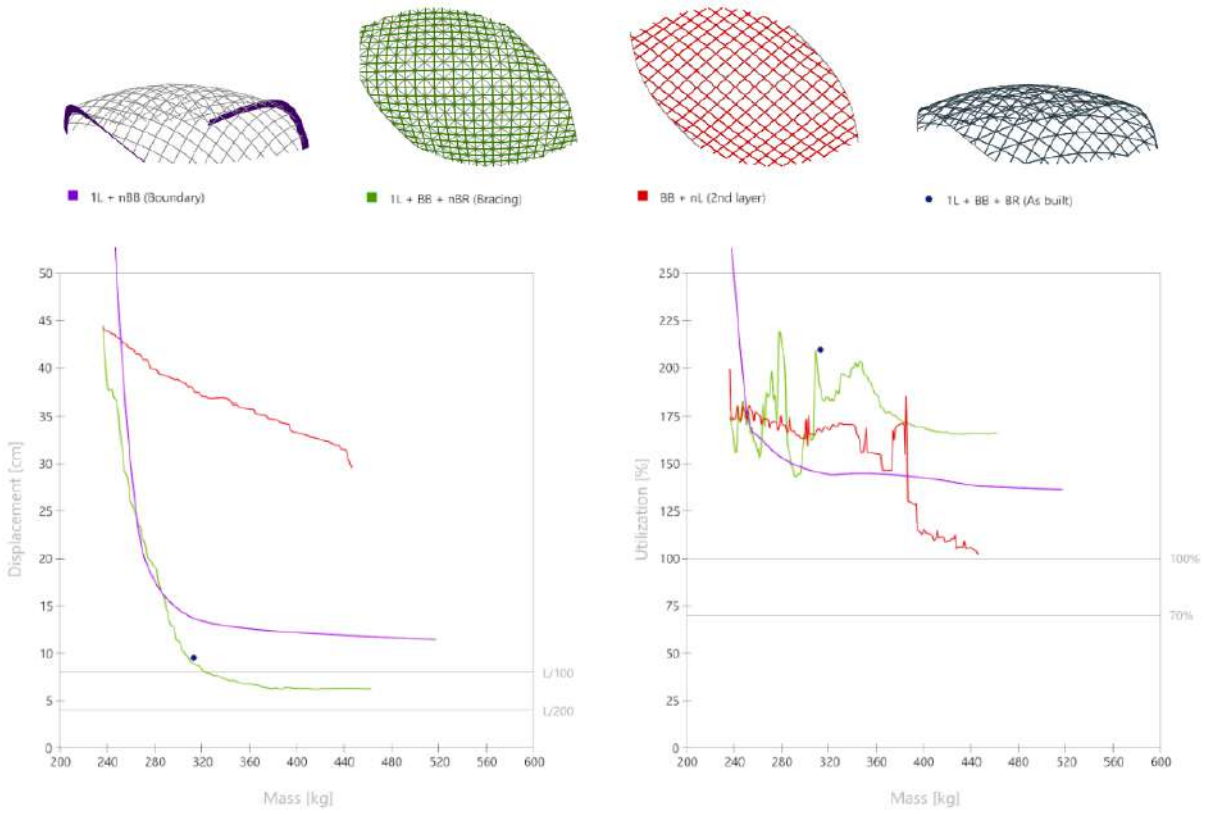

Figure 22: Comparison of the impact of the individual members on the displacement and the utilization.

Comparing the individual members' impact on the utilization it becomes apparent that the boundary beams are very effective to decrease the utilization at first. Further, the utilization remains almost constant within the grid. Adding the bracing elements results in local peaks and the utilization stays at high values. The same can be noticed for adding second layers, but they tend to decrease the utilization in general. Individually, with none of these members the maximum utilization of 70% is met.

3.3. Combinations and Final Comparisons

In order to increase the structural performance so that both the limit of displacement and utilization are met, a process is designed to efficiently combine the before-presented optimization algorithms.

3.3.1. Combination 1 - Optimization of all members

Within the first combination, all of the individual members are optimized. Therefore, the optimization process starts from a single-layer grid without any bracing. First, the stiffness of the boundary beams is increased until reaching the inflection point of the curve. Following, the utilization of the bracing elements is determined according to Chapter 3.2.2. which are then added sequentially until the maximum limit of displacement (*L/200*) is met. Based on the optimized boundary beams and resulting bracing pattern, second layers are finally added to reduce the utilization to a value of 70%. A detailed flowchart of this algorithm can be reviewed in Appendix A.4.

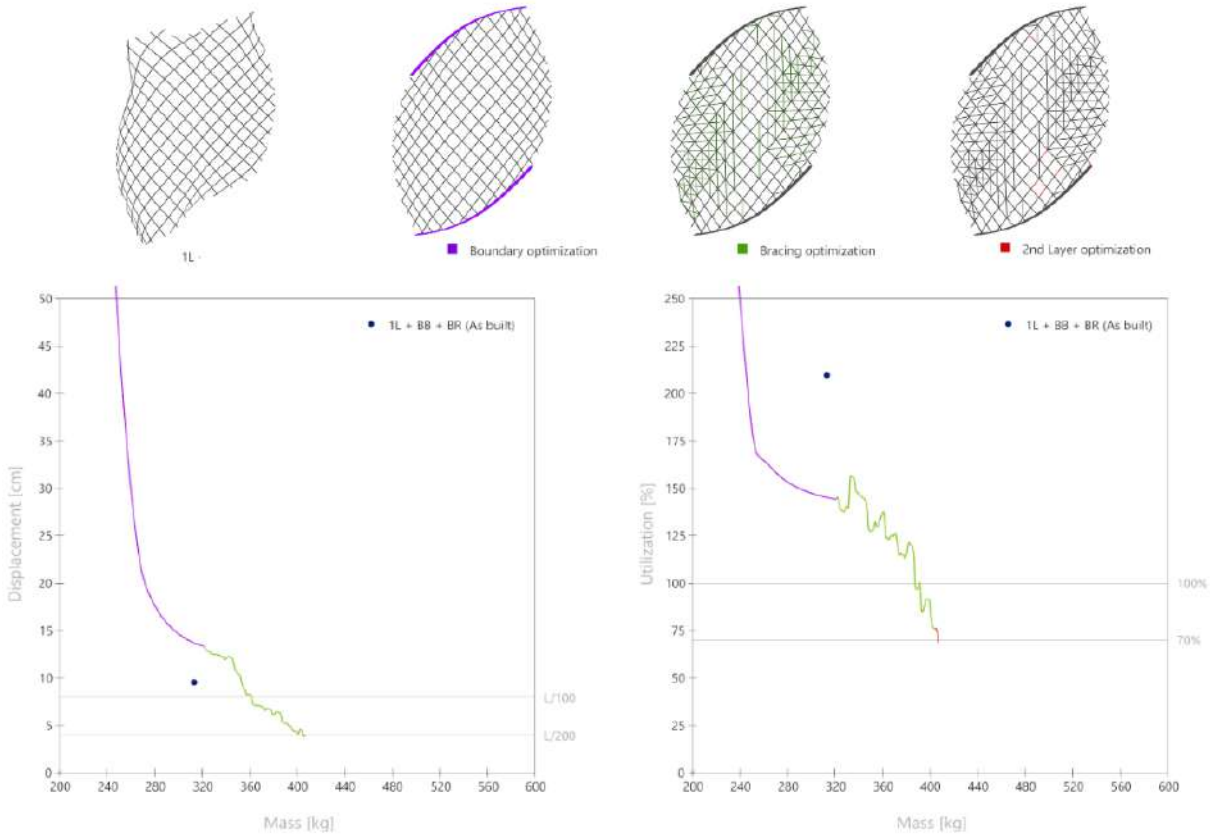

Figure 23: Optimization process and final results for combination 1

These individual steps are illustrated in Figure 23. By increasing the stiffness of the boundary beams, both the displacement and the utilization decrease. The bracing then reduces the displacement to the desired value. Here again, an interesting pattern with rotational symmetry of vertical and horizontal elements emerges. At this point, the defined limit of utilization is almost reached. Very few elements of the second layer help to reduce it to the desired value.

From a manufacturing point of view, bracing the structure with many short elements of different lengths is time-consuming. As seen in the intermediate comparisons of Chapter 3.2.4., the built bracing is already performing very efficiently. Therefore a second combination is built, starting from the built bracing of long continuous laths.

3.3.2. Combination 2 - Optimization based on the built bracing

Within the second combination, the optimization process starts from a single-layer grid that is braced as built. Here, the stiffness of the boundary beams is increased until reaching the maximum limit of displacement (*L/200*). Following this, second layers are added to reduce the utilization to a value of 70%. A detailed flowchart of this algorithm can be reviewed in Appendix A.5.

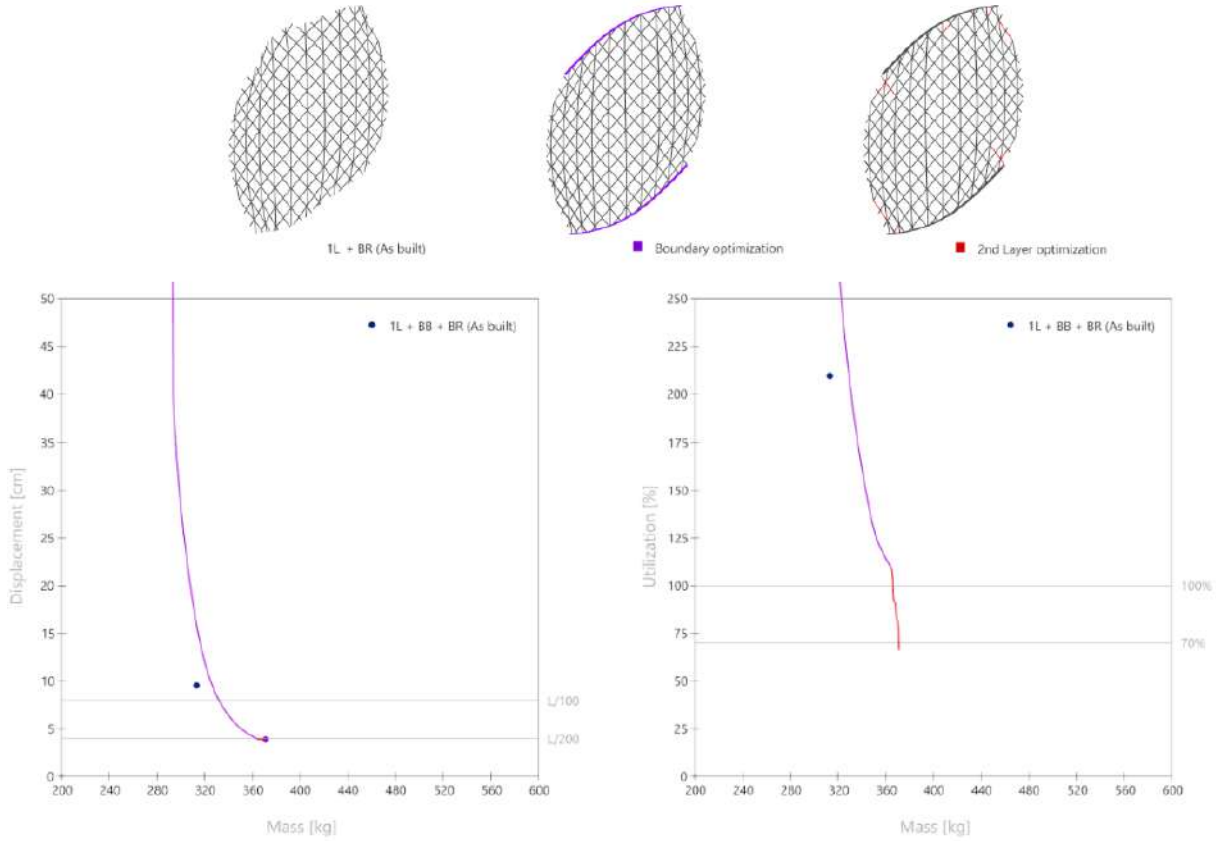

Figure 24: Optimization process and final results for combination 2

It becomes apparent that by increasing the stiffness of the boundary beams, which accounts only for about 60,0 kg of additional weight, the maximum limit of displacement (*L/200*) is already met. Again, very few elements of the second layer are needed to reduce the utilization to the desired value. These elements tend to be at the supports near the openings.

3.3.3. Final Comparisons

Finally, the different combinations are compared with each other. Figure 25 shows therefore the structure as built, with a complete second layer or bracing, and optimized within combinations 1 and 2.

It can be seen that the ones that are optimized within combinations 1 and 2, both meet the maximum limit of displacement (*L/200*) and utilization (70%) with a similar amount of applied mass.

By adding a complete second layer or bracing, the displacement is within an acceptable range between the minimum and the maximum limit. However, a lot of mass needs to be applied. Only by adding a complete second layer, also the limit of utilization is met.

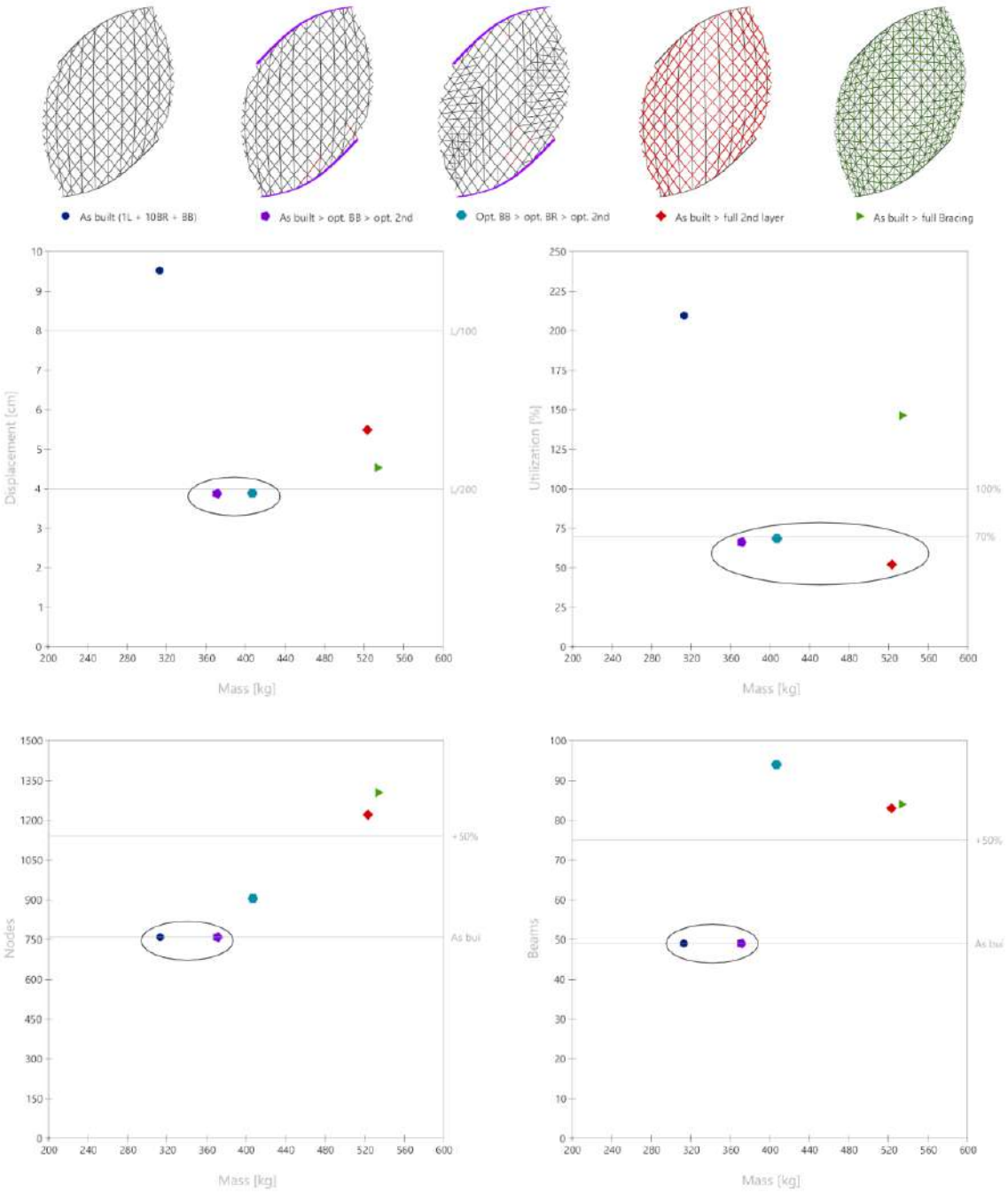

Figure 25: Final comparison of the structural performance and required manufacturing and assembly time.

To compare the different combinations in terms of manufacturing and assembly time, this figure also shows the resulting number of nodes and beams in relation to the mass applied.

One can see that adding a complete second layer or bracing, obviously leads to a considerable increase of nodes and beams. Since many short elements are added within combination 1, the number of nodes rises slightly, whereas the number of beams rises significantly, compared to the structure with long continuous laths. This requires more time for manufacturing and assembly.

It is the structure optimized within combination 2 that gives the best results. With only a few more nodes and beams to be assembled and manufactured compared to the built structure, the performance can be increased to meet both the limit of displacement and utilization.

As the boundary beams are following the geodesic curves, the width of the beams can be increased to 12,0 cm. With an intermediate layer of additional shear blocks, the height can be increased to 12,6 cm. This corresponds to the required stiffness of the cross-section.

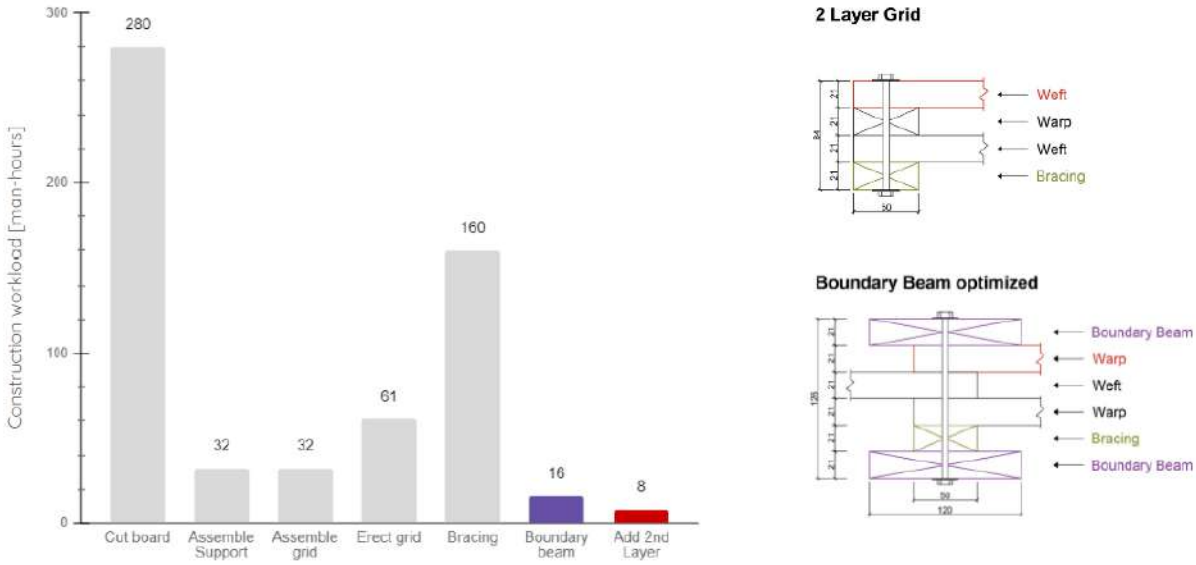

Figure 26: Required workload (colored) and construction details for the final improvement of the built structure.

4. Conclusions and Further Research

4.1. Conclusions

The structural performance of the presented single-layer elastic gridshell can be mainly improved by reinforcing the openings with stiff boundary beams. This is essential for gridshells with big openings.

For small-scale elastic gridshells made of timber, the simplicity of single-layer gridshells can be maintained, by reinforcing with a second layer only certain areas of high utilization.

It can be stated that with an efficient arrangement of bracing elements, around 50% of the potentially available quantity is already decreasing the displacement up to a point where adding more elements doesn't have much of an impact. Bracing the structure with an optimized pattern of short elements is not more efficient than bracing with a regular pattern of long elements. There is a similar performance compared to a similar amount of additional weight while requiring more time for manufacturing and assembling.

4.1. Further Research

The developed optimization algorithms should be applied to different shapes to validate the obtained results for their generality. Thereby, the phenomenon of buckling should also be taken into account.

Furthermore, the impact of additional parameters, such as varying the grid density or cross-section, needs to be investigated.

References

[1] Haskell, Charles & Montagne, Nicolas & Douthe, Cyril & Baverel, Olivier & Fivet, Corentin. (2021). Generation of elastic geodesic gridshells with anisotropic cross sections. International Journal of Space Structures. 36.

[2] Hernández, Elisa & Baverel, Olivier & Gengnagel, Christoph. (2013). On the Design and Construction of Elastic Gridshells with Irregular Meshes. International Journal of Space Structures. 28.

[3] Masson, Yannick. (2017). Existence and construction of Chebyshev nets with singularities and application to gridshells. Université Paris-Est. Ecole des Ponts ParisTech. Ph.D. Thesis

[4] D'Amico, Bernardino. (2013). Form-finding and structural optimization of timber grid-shell structures. Edinburgh Napier University. Ph.D. Thesis

[5] B. D'Amico & A. Kermani & H. Zhang & A. Pugnale & Colabella & S. Pone. (2015). Timber gridshells: Numerical simulation, design and construction of a full scale structure. Napier University. Ph.D. Thesis

[6] Accoya® timber gridshell, 2014, *Karamba 3D website,* accessed 10 September 2022, <https://www.karamba3d.com/project/accoya-timber-gridshell/>

[7] Portalen Pavillion, 2019, *Summum Engineering website*, accessed 10 September 2022, <https://www.summum.engineering/portfolio/portalen/>

[8] Aleš, Vaněk. (2018). Architectural solution of single-layer membrane integration into gridshell structures. Czech Technical University. Ph.D. Thesis

[9] UPM-Kymmene Corporation. (2007). Handbook of Finnish Plywood. Finnish Forest Industries Federation (Lahti, Finland: Kirjapaino Markprint Oy)

[10] Lienhard, Julian. (2014). Bending-active structures: form-finding strategies using elastic deformation in static and kinetic systems and the structural potentials therein. Universität Stuttgart. Ph.D. Thesis

[11] Lara-Bocanegra, Antonio José & Majano-Majano, Almudena & Arriaga, Francisco & Guaita, Manuel. (2018). Long-term bending stress relaxation in timber laths for the structural design of lattice shells. Construction and Building Materials. 193. 565-575.

A. Appendix

A.1. Flowchart of the boundary beam optimization algorithm

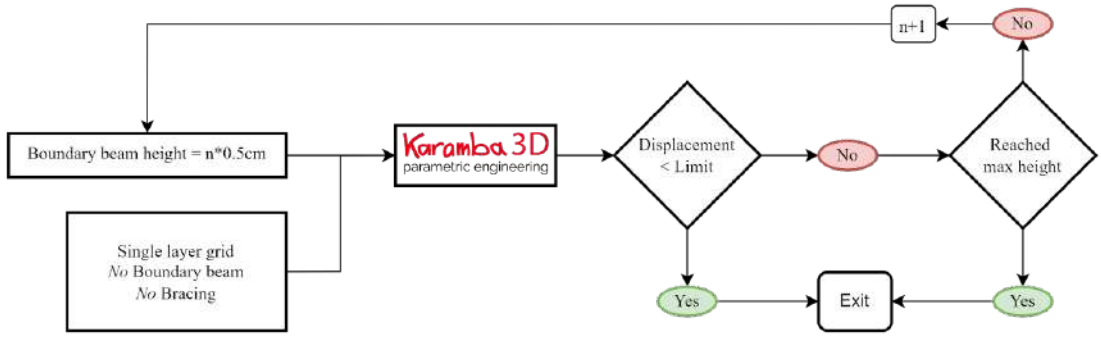

A.2. Flowchart of the bracing optimization algorithm

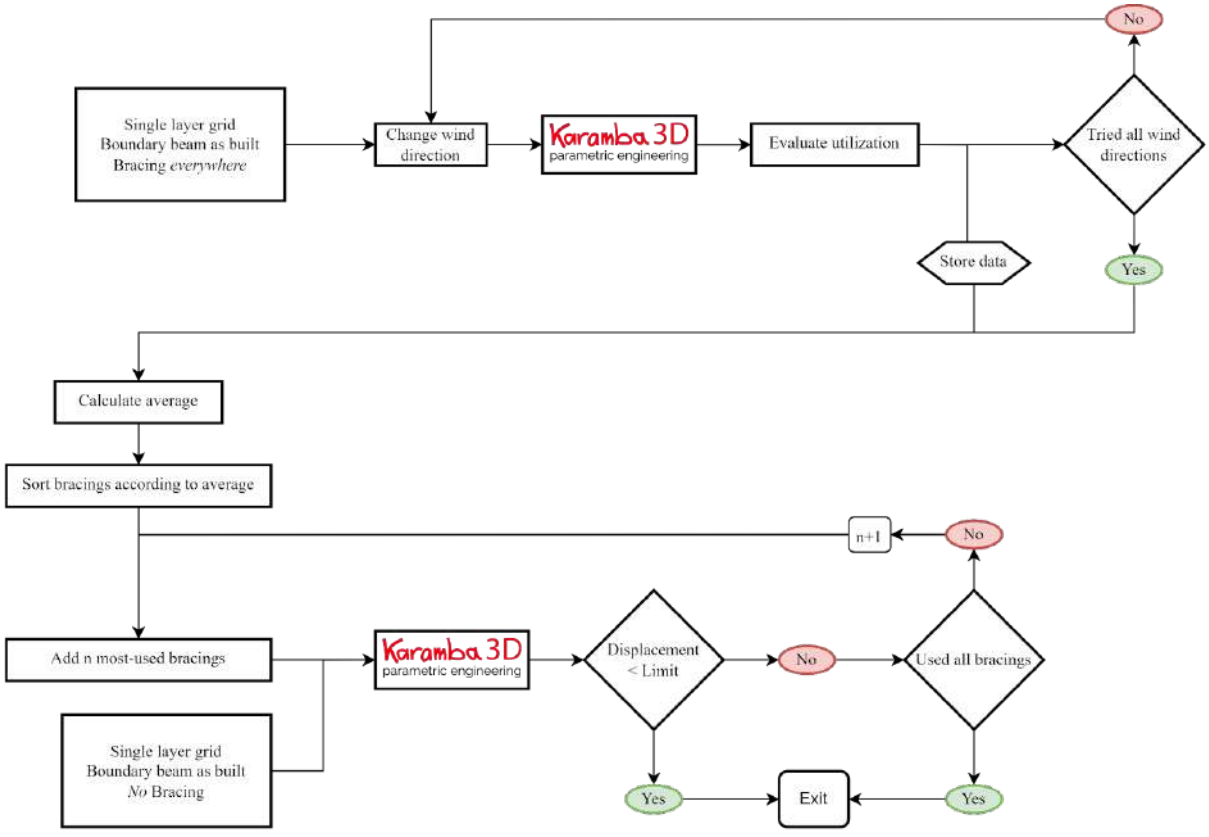

A.3. Flowchart of the second layer optimization algorithm

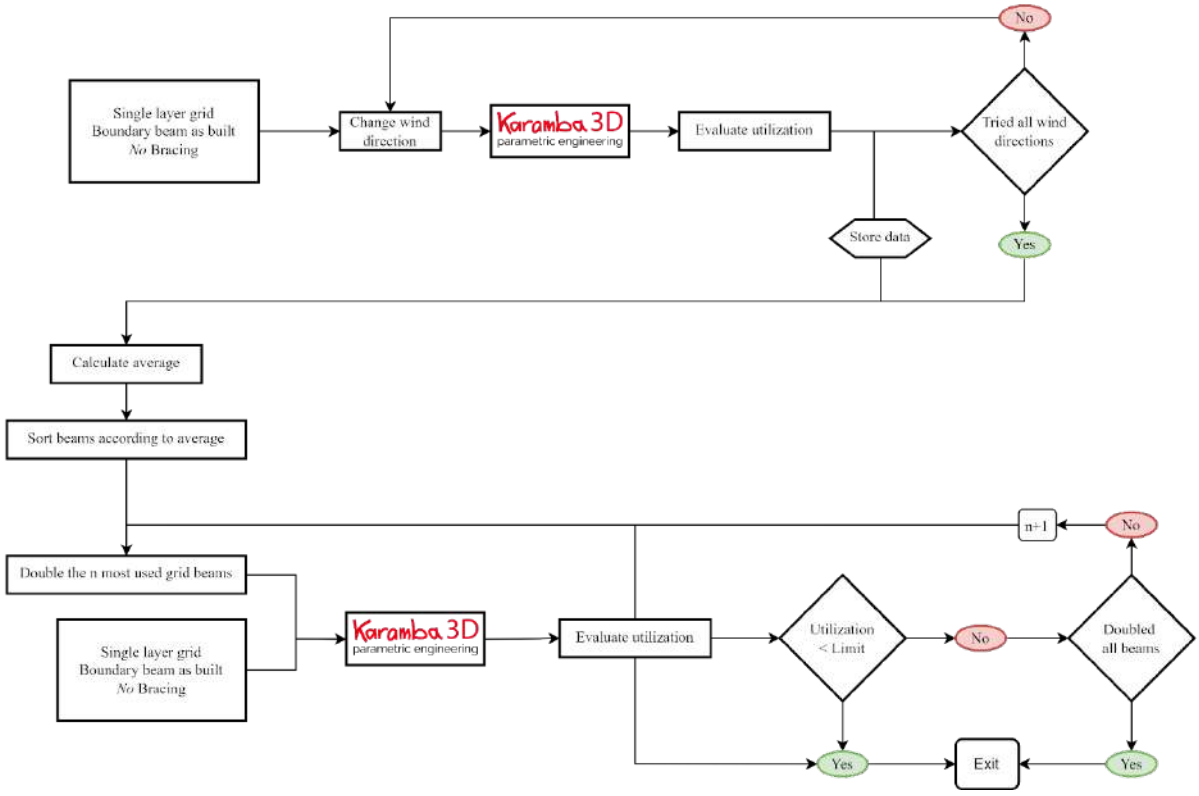

A.4. Flowchart of the optimization algorithm for combination 1

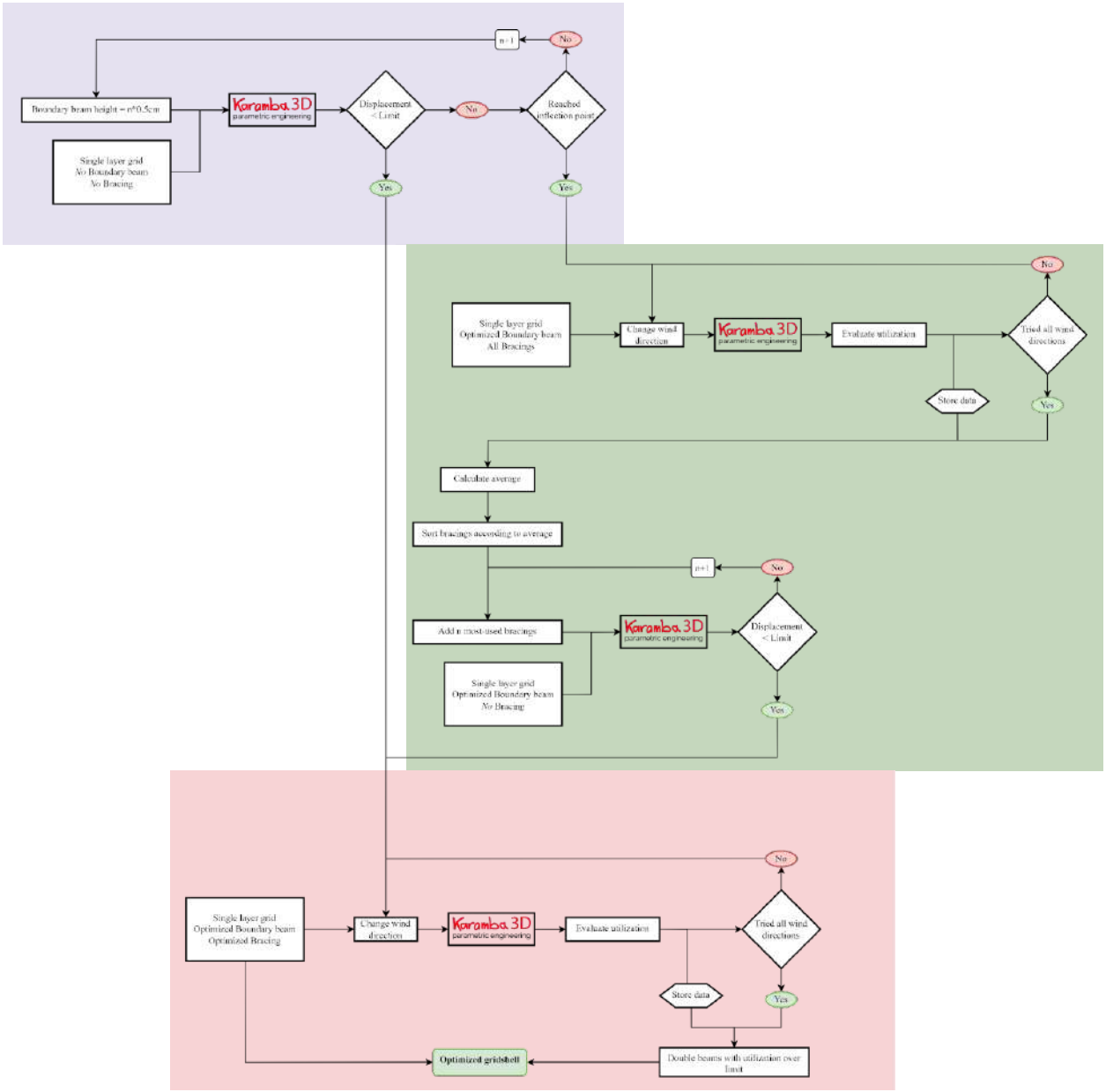

A.5. Flowchart of the optimization algorithm for combination 2